12^{th} International Conference on Fracture Mechanics of Concrete and Concrete Structures
FraMCoS-12
B.L.A. Pichler, Ch. Hellmich, P. Preinstorfer (Eds)

https://doi.org/10.21012/FC12.1351
TT-G:5

PREDICTION OF FATIGUE CRACK GROWTH IN ROCK-CONCRETE INTERFACE

VEREASH CHANDER SHARMA*, K.M. PERVAIZ FATHIMA†

Indian Institute of Technology Jammu, JK India
*e-mail: 2023pte0076@iitjammu.ac.in
†e-mail: pervaiz.khatoon@iitjammu.ac.in

Key words: Rock Concrete Interface, Paris Law, Mode Mixity, Interface Fracture, Fatigue Loading

Abstract. Rock-concrete interface is found in various engineering structures such as dams, tunnels, bridge piers etc. These structures are subjected to cyclic loading resulting in fatigue. Interface is the weakest and the most critical zone which is susceptible to crack formation and propagation. Understanding the effect of fatigue loading on the rock-concrete interface is useful in predicting the service life of these structures which ultimately ensures the durability of the structure. However, the heterogeneity that lies between rock and concrete poses significant challenge in analyzing the effect of fatigue crack growth at the interface. Further, as seen from the literature the fatigue test data exhibit an enormous scatter due to the inherent variability in the fatigue strength of the material as well as the statistical nature of the load experienced by them. Hence, for a reliable fatigue life estimation a deterministic approach is not sufficient. This paper proposes a generalized model derived from Paris' law to predict fatigue crack propagation in the rock-concrete interface. Additionally, it employs a probabilistic approach to estimate the fatigue life of the interface. In order to incorporate the heterogeneity at the interface, effective Young's modulus is used. The inherent mixed mode condition is included in the Paris' law through the stress intensity factors in both mode I and mode II. The crack propagation as a function of number of load cycles is predicted and the same is validated using available experimental results.

1 INTRODUCTION

The rock-concrete interface is a predominant feature of various large-scale structures such as gravity dams, offshore structures, tunnels, etc. and this interface acts as a potential site for crack formation and propagation. These structures are subjected to cyclic loading which gradually reduces the structure's stiffness, ultimately resulting in failure. The behavior of the bi-material interface under fatigue loading is more complex as compared to concrete or rock alone. This complexity is because of the mismatch in the parameters such as elastic modulus, thermal expansion etc. which makes the stress field complex in nature.

A review of the past studies highlights the dependence of interfacial fracture behavior on the mode mixity ratio. For instance, Slowik et al. [11] observed that under mixed-mode loading, interfacial cracks tend to kink into the adjoining material, illustrating the critical role of loading conditions. Similarly, Yang et al. [4] studied single-notched concrete-rock beams and reported that Mode I fracture toughness at the interface is significantly influenced by the mode mixity ratio. Moreover, various studies [3, 5] reveal that the mechanical and fracture behavior of the interface are strongly affected by its roughness. A smoother interface tends to exhibit a more extensive fracture process zone,

while increased roughness leads to higher brittleness and a reduction in the process zone size [13].

Considerable efforts have been directed in the past for predicting fatigue crack growth in concrete. For example, Bazant and his group [1, 2] introduced a size adjusted model for fatigue crack propagation in concrete by incorporating transitional sizes into the traditional Paris' law framework. Shah et al. [10] examined the fatigue crack behavior in the concrete-concrete interface and derived an analytical model for predicting the fatigue crack growth using the principle of dimensional analysis. Zhao et al. [14] used the adjusted Paris' law to predict the fatigue crack growth in rock-concrete interface. However, loading condition as pure mode I.

Moreover research related to understanding the fatigue crack growth in bi-material interface is primarily experimental and mostly limited to concrete-concrete interface. Due to the intrinsic heterogeneity in strength across different materials, a significant scatter has also been observed in the fatigue life prediction in these experiments. In line with this, the objectives of this research are to predict fatigue crack growth in the rock-concrete interface using a modified version of Paris' law and also estimate fatigue life using a probabilistic distribution model.

2 MECHANICS OF INTERFACE CRACK

A crack that initiates at an interface may kink into one of the materials or grow along the interface. The relative toughness of the interface and the material on either side of the interface determine whether a crack is compelled to stay along the interface or kink. For a bi-material interface crack shown in Figure 1, the near tip normal (σ_{yy}) and shear stresses (τ_{xy}) are given by [7].

$$\sigma_{yy} + i\tau_{xy} = \frac{(K_I + iK_{II})r^{i\epsilon}}{(2\pi r)} \quad (1)$$

where i=$\sqrt{-1}$, K_I and K_{II} are the components of complex stress intensity factor K= K_I + iK_{II} and ϵ is the oscillation index given by

$$\epsilon = \frac{1}{2\pi} \ln\left(\frac{1-\beta}{1+\beta}\right) \quad (2)$$

where β is one of Dunder's [6] elastic mismatch parameters, which for plane strain is given by

$$\beta = \frac{\mu_1(1-2\nu_2) - \mu_2(1-2\nu_1)}{2[\mu_1(1-\nu_2) + \mu_2(1-\nu_1)]} \quad (3)$$

Here, μ and ν represent the shear modulus and Poisson's ratio, respectively, with the subscripts 1 and 2 denoting the materials above and below the interface.

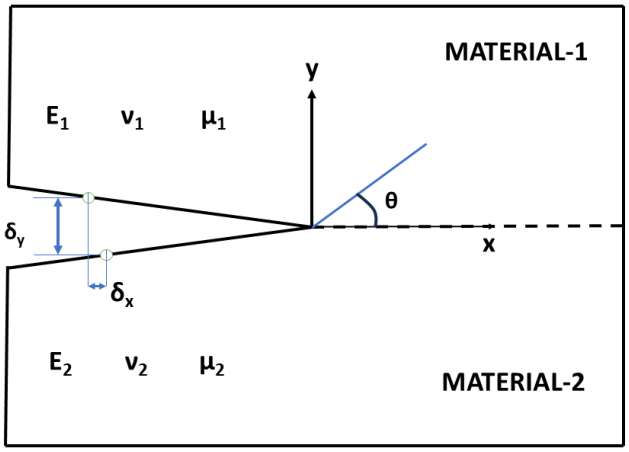

Figure 1: Illustration of a bi-material interface crack

When the material above and below the interface are the same then β and ϵ vanish. The stresses exhibit significant oscillations as the fracture tip approaches ($r \rightarrow 0$), as seen in Equation (1) when $\epsilon \neq 0$. In a bi-material interface, due to the component $r^{i\epsilon}$, the balance between normal and shear stresses near the crack tip changes gradually with the radial distance. Unlike in a homogeneous material fracture, the stress intensity factors K_I and K_{II} cannot be distinctly separated to represent the normal and shear stress intensities. This leads to a mix of fracture modes, known as mode-mixity.

3 PREDICTION MODEL FOR FATIGUE CRACK

Paris' law [9], which is one of the most widely used fatigue crack propagation models

expresses the rate of fatigue crack growth per load cycle as a function of the stress intensity factor range and is mathematically stated as

$$\frac{da}{dN} = C(\Delta K)^m \quad (4)$$

where a represents the crack length, N indicates the number of load cycles; ΔK denotes the stress intensity factor range, C and exponent m denote material constants. In order to predict fatigue crack growth in a bi-material interface which inherently shows mode mixity, the traditional Paris' law has been modified by introducing equivalent stress intensity factor ΔK_{eq} as illustrated in Equation 5

$$\frac{da}{dN} = C(\Delta K_{\text{eq}})^m \quad (5)$$

Different forms of ΔK_{eq} are available in the literature. One such formulation, based on Irwin's energy concept [8] for mixed-mode fracture, is being used in this work:

$$\Delta K_{\text{eq}} = \left(\Delta K_I^2 + \Delta K_{II}^2\right)^{1/2} \quad (6)$$

where ΔK_I and ΔK_{II} are the interfacial stress intensity factor range for mode I and mode II respectively where K_I for three point bending specimen was given by Tada et al. [12],

$$K_I = \frac{3PS}{2D^2B}(\sqrt{a})F_1(\frac{a}{D}) \quad (7)$$

where P is the applied load, S is the span, D and B are the specimen height and width respectively. $F_1(\frac{a}{D})$ is a dimensionless correction factor that accounts for the geometry of the specimen and the relative crack depth $\frac{a}{D}$ and is given as

$$F_1\left(\frac{a}{D}\right) = \frac{1.99 - \left(\frac{a}{D}\right)\left(1 - \frac{a}{D}\right)(\gamma)}{(1 + 2\frac{a}{D})(1 - \frac{a}{D})^{1.5}} \quad (8)$$

where γ is

$$\gamma = 2.15 - 3.93\left(\frac{a}{D}\right) + 2.7\left(\frac{a}{D}\right)^2$$

As the geometric factor mentioned above applies to homogeneous materials, a correction function F_2 [13] is introduced to account for the influence of elastic mismatch at the bi-material interface and the specimen size where,

$$F_2\left(\frac{E_2}{E_1}, \frac{a}{D}\right) = Q_1 + Q_2\left(\frac{E_2}{E_1}\right) + Q_3\left(\frac{E_2}{E_1}\right)^2 \quad (9)$$

$$Q_1 = 0.975 + 0.074\left(\frac{a}{D}\right) - 0.062\left(\frac{a}{D}\right)^2 \quad (10)$$

$$Q_2 = 0.023 - 0.067\left(\frac{a}{D}\right) + 0.056\left(\frac{a}{D}\right)^2 \quad (11)$$

$$Q_3 = -0.001 + 0.003\left(\frac{a}{D}\right) - 0.002\left(\frac{a}{D}\right)^2 \quad (12)$$

The stress intensity factor in Equation (7) is thus modified as:

$$K_I^* = K_I F_1\left(\frac{a}{D}\right) F_2\left(\frac{E_2}{E_1}\right) \quad (13)$$

In order to develop a prediction model for fatigue crack growth in rock-concrete interface the experimental data provided by the Zhao et al. [14] has been utilized. Rock-concrete beams were tested under three point bending using two loading schemes. In scheme 1, P_{min} was fixed and P_{max} was varied and in scheme 2, P_{max} was fixed and P_{min} was varied. The granite-concrete interface was cyclically loaded with P_{max} equal to $\text{Y}\%(P_u)$ and P_{min} equal to $\text{Z}\%(P_u)$, indicated by the FGX-Y-Z symbol, where X represents the grade of concrete. Here, P_u indicates peak load under monotonic loading. For example FG30-85-2-1 represents concrete grade of 30, the maximum load of $85\%(P_u)$, minimum load of $2\%(P_u)$ and 1 represents the specimen number. The material properties for rock and concrete are presented in Table 1 and material constants C and m for different specimens are shown in Table 2

Table 1: Mechanical properties of concrete and rock [14].

Material	E (GPa)	$\boldsymbol{\nu}$	f_c (MPa)
Rock Granite	43.89	0.17	87.91
Concrete C60	44.01	0.23	72.09
Concrete C40	39.36	0.20	55.72
Concrete C30	36.02	0.21	44.85

Table 2: Values of m and C for all the tested specimens [14].

Specimen No.	m	C
FG30-85-2-1	16.371	2.753
FG30-85-2-2	15.218	4.966
FG30-85-2-3	20.805	5.154
Mean value	**17.465**	**4.291**
FG40-85-2-1	20.854	3.439
FG40-85-2-2	15.764	2.366
FG40-85-2-3	19.751	3.758
Mean value	**18.790**	**3.188**
FG60-90-2-1	22.521	1.981
FG60-90-2-2	15.259	0.655
FG60-90-2-3	21.847	1.413
Mean value	**19.876**	**1.350**
FG60-95-2-1	25.536	2.379
FG60-95-2-2	19.092	1.649
FG60-95-2-3	15.095	1.315
Mean value	**19.908**	**1.781**

Based on these experimental data, the modified model is used for predicting mixed-mode fracture. Separating variables of Equation (5) we have,

$$dN = \frac{1}{C(\Delta K_{eq})^m} da \tag{14}$$

Equation (14) is then integrated from N_i to N_{i+1} as crack length increases from a_i to a_{i+1} and this process is repeated in an incremental manner until number of load cycles to failure N_f and corresponding critical crack length a_c is achieved.

$$\int_{N_i}^{N_{i+1}} dN = \int_{a_i}^{a_{i+1}} \frac{1}{C(\Delta K_{eq})^m} da \tag{15}$$

The right hand side of Equation 15 has been integrated using the integration by limit of sum method:

$$N(f) = (a_{i+1} - a_i) \lim_{n\to\infty} \frac{1}{n} \sum_{a=a_i}^{a_{i+1}} \frac{1}{C(\Delta K_{eq})^m} \tag{16}$$

Equation (16) provides the number of load cycles corresponding to the crack length increment from a_i to a_{i+1}. Crack length versus number of load cycles is then plotted.

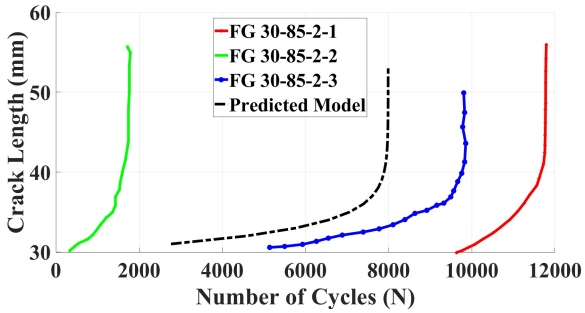

Figure 2: Crack length versus number of load cycles (N) for FG30-85-2

Figures 2, 3, 4 and 5 illustrate the relation between crack length and the number of load cycles under different loading conditions. The predicted model results exhibit a good match with the experimental data reported by Zhao et al. [14].

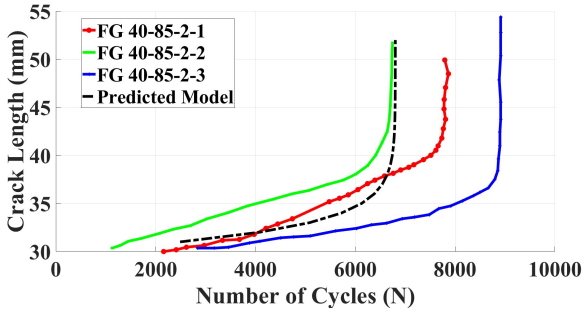

Figure 3: Crack length versus number of load cycles (N) for FG40-85-2

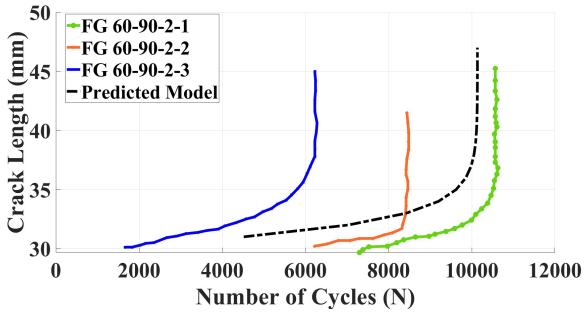

Figure 4: Crack length versus number of load cycles (N) for FG60-90-2

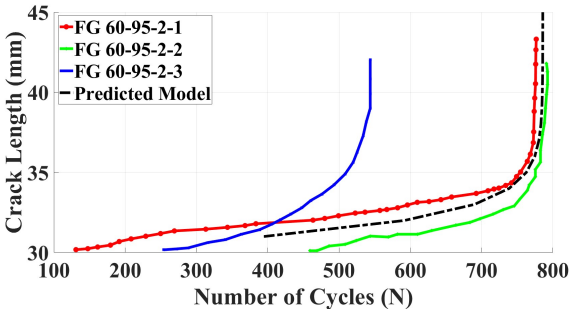

Figure 5: Crack length versus number of load cycles (N) for FG60-95-2

4 PROBABILISTIC APPROACH FOR FATIGUE LIFE PREDICTION

According to the experimental study by Zhao et al. [14], there is a significant amount of variation in the specimen fatigue life data as seen in Table 3. A probabilistic model for evaluating the fatigue life of the rock-concrete interface is presented here.

Table 3: Comparison of experimental data with the predicted data

Specimen No.	Number of Cycles to Failure (Experimental) [14]	Average Experimental Cycles to failure	Predicted Fatigue Life	% Error
FG30-85-2-1	11792			
FG30-85-2-2	1718	7772	7900	1.646
FG30-85-2-3	9806			
FG40-85-2-1	7792			
FG40-85-2-2	6746	7817	7750	0.85
FG40-85-2-3	8912			
FG60-90-2-1	1216			
FG60-90-2-2	1450	1215	1226	0.90
FG60-90-2-3	980			
FG60-95-2-1	776			
FG60-95-2-2	790	703	700	0.42
FG60-95-2-3	543			

The probabilistic fatigue life of rock-concrete specimens was predicted using a Monte Carlo simulation approach based on the modified Paris' law given in Equation (17). To account for the variability in C and m, experimental data for these parameters were used to fit statistical distributions. The parameter C was assumed to follow a log-normal distribution, while m followed a normal distribution. The fatigue life (N_f) for each Monte Carlo realization was computed by numerically integrating the crack growth equation over a range of crack increments:

$$N_\mathrm{f} = \int_{a_0}^{a_f} \frac{1}{C\left(\Delta K_\mathrm{eq}\right)^m}\, da, \qquad (17)$$

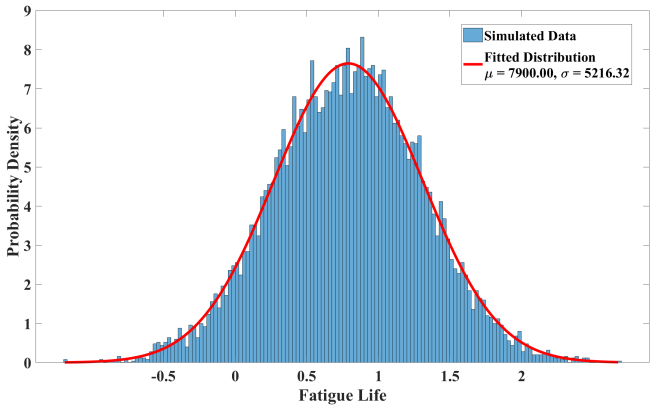

Figure 6: Simulated fatigue life of FG30-85-2

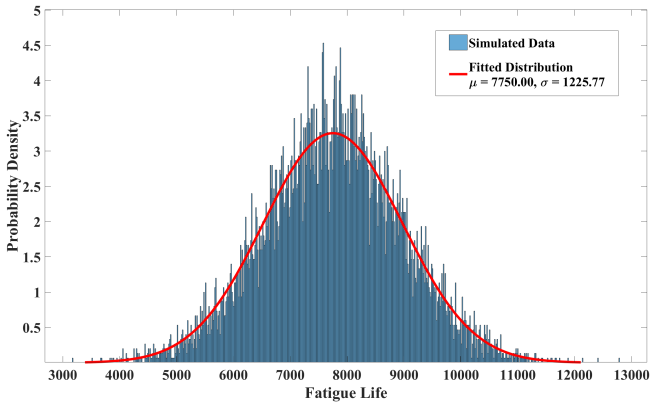

Figure 7: Simulated fatigue life of FG40-85-2

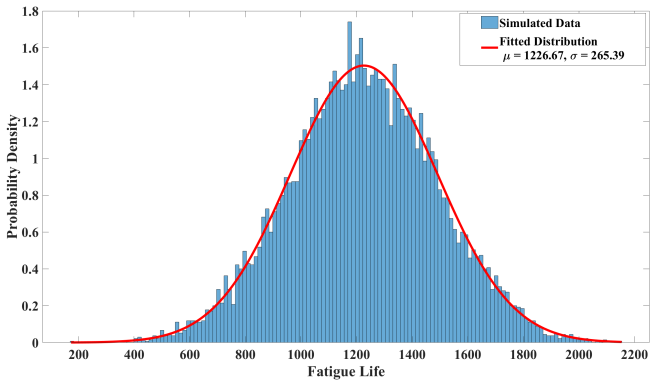

Figure 8: Simulated fatigue life of FG60-90-2

where a_0 and a_f represent the initial and final crack lengths. Initial crack length is taken as the

initial notch length which is 30 mm in this work, while final crack length is crack length corresponding to the failure of the beams obtained through the fatigue experiments. The simulated fatigue life for 10000 simulations is plotted in Figures 6, 7, 8 and 9 which correspond to specimens FG30-85-2, FG40-85-2, FG60-90-2 and FG60-95-2 respectively. The plot shows a probability density function (PDF) for the simulated fatigue life (N_f) , represented by the histogram overlaid with a fitted distribution curve. The fatigue life data follows a bell-shaped distribution, likely a normal (Gaussian) distribution, as indicated by the smooth curve. The experimental data generally lie close to the peak of the simulated distribution, suggesting that the simulation captures the central behavior of the material's fatigue life well. The histogram indicates some spread in the simulated data, which aligns with the variability in fatigue life due to material and experimental uncertainties.

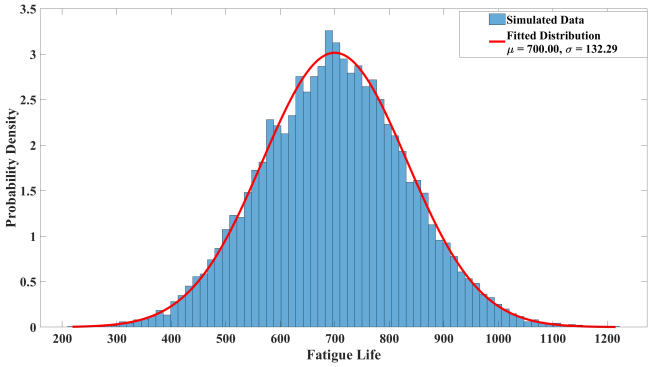

Figure 9: Simulated fatigue life of FG60-95-2

5 CONCLUSION

This study presents a generalized model derived from Paris' law, where the equivalent stress intensity factor (ΔK_{eq}) has been used in the place of the general mode-I stress intensity factor in an effort to integrate the mixed mode character of the rock-concrete interface. A large scatter in fatigue life is observed in the experimental data, hence a probabilistic model for predicting fatigue life using Monte Carlo simulation is presented. The results of the proposed probabilistic model were compared with the available experimental data and were found to be in good agreement.

References

[1] Bazant, Z. P. and Schell, W. F. [1993], 'Fatigue fracture of high-strength concrete and size effect', *ACI Materials Journal* **90**, 472–472.

[2] Bazant, Z. P. and Xu, K. [1991], 'Size effect in fatigue fracture of concrete', *ACI Materials Journal* **88**(4), 390–399.

[3] Dong, W., Wu, Z. and Zhou, X. [2016], 'Fracture mechanisms of rock-concrete interface: Experimental and numerical', *Journal of Engineering Mechanics* **142**(7), 04016040.

[4] Dong, W., Yang, D., Zhang, B. and Wu, Z. [2018], 'Rock-concrete interfacial crack propagation under mixed mode i-ii fracture', *Journal of Engineering Mechanics* **144**(6), 04018039.

[5] Dong, W., Yang, D., Zhou, X., Kastiukas, G. and Zhang, B. [2017], 'Experimental and numerical investigations on fracture process zone of rock–concrete interface', *Fatigue & Fracture of Engineering Materials & Structures* **40**(5), 820–835.

[6] Dundurs, J. [1969], 'Discussion: Edge-bonded dissimilar orthogonal elastic wedges under normal and shear loading', *Journal of Applied Mechanics* **36**(3), 650–652.

[7] Hutchinson, J. W. and Suo, Z. [1991], 'Mixed mode cracking in layered materials', *Advances in Applied Mechanics* **29**, 63–191.

[8] Irwin, G. R. [1957], 'Analysis of stresses and strains near the end of a crack traversing a plate', *Journal of Applied Mechanics* **24**(3), 361–364.

[9] Paris, P. and Erdogan, F. [1963], 'A critical analysis of crack propagation laws', *Journal of Basic Engineering* **85**(4), 528–533.

[10] Shah, S. G., Ray, S. and Kishen, J. C. [2014], 'Fatigue crack propagation at concrete–concrete bi-material interfaces', *International Journal of Fatigue* **63**, 118–126.

[11] Slowik, V., Kishen, J. C. and Saouma, V. E. [1998], 'Mixed mode fracture of cementitious bimaterial interfaces;: Part i: Experimental results', *Engineering Fracture Mechanics* **60**(1), 83–94.

[12] Tada, H., Paris, P. C. and Irwin, G. R. [1973], 'The stress analysis of cracks', *Handbook, Del Research Corporation* **34**(1973).

[13] Yuan, W., Dong, W., Zhang, B. and Zhong, H. [2021], 'Investigations on fracture properties and analytical solutions of fracture parameters at rock-concrete interface', *Construction and Building Materials* **300**, 124040.

[14] Zhao, X., Dong, W. and Li, S. [2024], 'Investigation on the fatigue crack propagation of rock-concrete interface under fatigue loading below the initial cracking load', *Engineering Structures* **315**, 118407.